Available online at www.sciencedirect.com

ScienceDirect

Structural Integrity Procedia 00 (2025) 000–000

Structural Integrity Procedia

www.elsevier.com/locate/procedia

XX ANIDIS Conference

UQ based state-dependent framework for recovery and seismic risk assessment

Chiara Nardin[a,b,*], Stefano Marelli[b], Bruno Sudret[b], Oreste S. Bursi[a], Marco Broccardo[a]

[a]*Department of Civil, Environmental and Mechanical Engineering, University of Trento, Trento 38122, Italy*
[b]*Chair of Risk, Safety and Uncertainty Quantification, ETH Zürich, Zürich 8093, Switzerland*

Abstract

Recovery processes and seismic risk assessment represent a critical and challenging frontier in engineering risk analysis under uncertainty. Despite growing attention, the problem remains inherently complex, shaped by nonlinear system behaviours and high-dimensional stochastic spaces. These difficulties are compounded by the limited availability and often confidential nature of recovery data, highlighting the urgent need for modelling approaches that are not only efficient, but also flexible enough to adapt to real-world constraints.

In this work, we introduce a novel framework that explicitly integrates recovery into state-dependent seismic risk assessment. The approach combines fragility modelling, recovery processes, and hazard evaluation into a cohesive structure, enabling holistic and reliable risk analysis. Designed for flexibility, the framework draws from the state-of-the-art in different disciplines, such as structural engineering, recovery modelling and probabilistic seismic modelling, and focuses on balancing adaptability and computational efficiency.

At the core of the methodology is a state-dependent seismic risk model that embeds recovery through a Continuous-Time Markov Chain (CTMC) framework. This enables the joint evaluation of damage progression and recovery over time. Spectral analysis of the reduced transition matrix allows for reliability-based metrics. The framework is applied to a full-scale industrial steel frame from the European SPIF project, tested under seismic loading at EUCENTRE, demonstrating its ability to capture resilience dynamics with computational efficiency.

Peer-review under responsibility of XX ANIDIS Conference organizers.

Keywords: Seismic risk assessment; state-dependent analysis; uncertainty quantification; polynomial chaos expansions; recovery functions

1. Introduction and Motivation

The PEER Performance-Based Earthquake Engineering (PBEE) framework has become fundamental in assessing how infrastructure systems respond to seismic events. Traditionally, however, its focus has been limited to outcomes such as damage, economic and life losses, often neglecting the recovery phase, which is central to true resilience.

* Corresponding author.
E-mail address: chiara.nardin@unitn.it, cnardin@ethz.ch

2210-7843
Peer-review under responsibility of XX ANIDIS Conference organizers.

Recovery dictates not just how a system survives, but how it adapts, maintains continuity, and supports decision-making in the aftermath of disaster.

Integrating recovery into PBEE is critical for industrial and strategic systems, where extended downtime can trigger wide-reaching disruptions across interconnected networks and supply chains. For such systems, resilience is inherently tied to both the severity of seismic hazard and the urgency of recovery. To illustrate this, we refer to a qualitative, PBEE-inspired resilience matrix (Figure 1) using five levels (very high to very low) to guide expected performance. For example, a “very high” resilience rating is demanded in contexts of high hazard and short required recovery, typical for essential services. Conversely, non-essential systems may tolerate long recovery under low hazard, warranting lower resilience expectations.

Despite the growing interest to the topic, as in the recent FEMA P-58 document (FEMA and NIST, 2021), REDi report Almufti and Willford (2013), and F-Rec tool Terzic et al. (2021), recovery modeling remains mostly fragmented, data-intensive, or narrowly scoped. This holds true especially in industrial domains, where downtime has widespread ripple effects, existing models struggle to generalize across assets or regions.

To address this, we propose embedding recovery directly within the PEER-PBEE framework using a Continuous-Time Markov Chain (CTMC) model. This approach captures the dynamic evolution of system states, allowing for probabilistic transitions conditioned on both damage level and seismic hazard intensity (e.g., return period). CTMCs offer a modular, uncertainty-compatible solution that aligns naturally with PBEE’s probabilistic hierarchy and is scalable even in data-scarce contexts.

Furthermore, this work introduces a reliability-inspired formulation for seismic resilience assessment. Specifically, we propose a metric grounded in a β-index, which relates both the hazard intensity and the expected time for the system to remain in a degraded state over its lifetime. This allows us to capture not just immediate failure probabilities, but the full dynamic behavior of a system through both degradation and recovery. As a result, we enable a rapid, robust, and quantitative assessment of system resilience, suitable for evaluating adaptation strategies and supporting recovery-centric design decisions.

The remainder of the paper is structured as follows. Section 2 outlines the core methodology driving our approach. Section 3 presents the case study and describes the key elements of the framework. Section 4 highlights preliminary findings and insights, while Section 5 offers concluding remarks and perspectives for future development.

Recovery Lead Time	Seismic Hazard Level: Low	Medium	High
Inst.	High	Very High	Very High
Short	High	High	Very High
Frequent	Medium	High	Very High
Medium	Medium	Medium	High
Long	Low	Medium	Medium

Legend: Very High, High, Medium, Low

Fig. 1. The PBEE-inspired resilience matrix adopted in this work

2. Theoretical Framework

Traditional risk assessments typically focus on preventing collapse under extreme events but often overlook the post-event phase, when survival, continuity, and recovery are paramount. Yet, understanding what happens after a disruption is essential for evaluating long-term system performance.

This section introduces a heuristic framework for system-level risk assessment that explicitly accounts for post-disaster recovery. Grounded in reliability theory and aligned with the PEER PBEE methodology, the framework integrates state-dependent fragility functions, CTMCs, and recovery models to evaluate both robustness and resilience.

Consider a system that can occupy one of three damage states: DS_0 (undamaged), DS_1 (slightly damaged), or DS_2 (collapsed). Hazard events, assumed to occur at a constant rate $\lambda_{IM,0}$, drive state transitions over the service life T_{Life} of the system.

Figure 2 illustrates the state diagram of the system. In this representation, the green-colored states correspond to the transient states (DS_0 and DS_1), while DS_2 denotes an absorbing state. An absorbing state is defined by the fact that, once entered, it cannot be exited. A CTMC framework models these transitions, capturing the stochastic evolution of

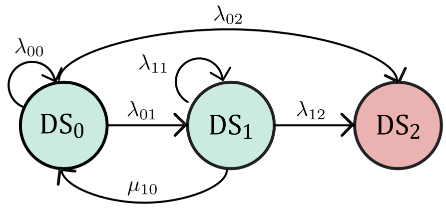

Fig. 2. State-diagram of the three-state system with an adsorbing state DS$_2$.

the system under repeated hazard and recovery.

Let $\boldsymbol{\pi}(t) = [\mathbb{P}_{\mathrm{DS0}}(t), \mathbb{P}_{\mathrm{DS1}}(t), \mathbb{P}_{\mathrm{DS2}}(t)]$ represent the time-dependent probability distribution over damage states. Its evolution follows:

$$\dot{\boldsymbol{\pi}}(t) = \boldsymbol{\pi}(t)\boldsymbol{Q}, \tag{1}$$

$$\boldsymbol{\pi}(t) = \boldsymbol{\pi}(0)\exp(\boldsymbol{Q}t), \tag{2}$$

where $\boldsymbol{Q}$ is the infinitesimal generator matrix, and Eq. (2) is the general analytical solution for the ordinary differential equation problem stated in Eq. (1). Various numerical and closed-form techniques are available to solve this equation; see, e.g., Trivedi and Bobbio (2017) for an overview.

Specifically, the generator matrix can be decomposed into two contributing terms, the seismic degradation ($\boldsymbol{Q}_{\mathrm{seis}}$) and recovery ($\boldsymbol{Q}_{\mathrm{rec}}$) sub-matrix, as:

$$\boldsymbol{Q} = \boldsymbol{Q}_{\mathrm{seis}} + \boldsymbol{Q}_{\mathrm{rec}} = \begin{bmatrix} -\sum_{j=0}^{2}\lambda_{0,j} & \lambda_{0,1} & \lambda_{0,2} \\ \mu_{1,0} & -\sum_{j=0}^{2} & \lambda_{1,2} \\ \mu_{2,0} & \mu_{2,1} & -\sum_{j=0}^{2}\mu_{2,j} \end{bmatrix}, \tag{3}$$

where the lower triangular matrix represents the recovery component, and the upper one represents the seismic damage component. It follows naturally that λ_{ij} represents the transition rate from state i to state j due to seismic events, and it can be evaluated using a PEER-PBEE-based formulation:

$$\lambda_{ij} = \int_{im} P(D = d_j | D = d_i, im) \left| \frac{d\lambda(im)}{dim} \right| dim, \tag{4}$$

Here, $\mathbb{P}(\mathrm{DS} = ds_j | \mathrm{DS} = ds_i, im)$ denotes the state-dependent probability of transitioning from damage state ds_i to ds_j given the intensity measure im, and $\lambda(im)$ is the exceedance rate of the im. Instead, at this stage, the recovery rates μ_{ij} are assumed to be constant and independent of both time and intensity measure.

As shown in Figure 2, DS$_2$ can represent an absorbing state. Meaning that once reached, it cannot be exited. In this case, the generator matrix can thus be partitioned as:

$$\boldsymbol{Q} = \begin{bmatrix} \boldsymbol{Q}_T & \boldsymbol{A} \\ 0 & 0 \end{bmatrix}, \tag{5}$$

where $\boldsymbol{Q}_T$ governs transitions between transient states. Moreover, spectral analysis of $\boldsymbol{Q}_T$ yields the quasi-stationary distribution (QSD)—the asymptotic distribution over the non-absorbing states (DS$_0$ and DS$_1$), conditioned on the system not having collapsed. The dominant eigenvalue λ_1 governs the rate at which probability mass leaks from the transient states into the absorbing state, effectively characterizing the decay rate toward collapse.

Additionally, the matrix $\boldsymbol{N} = (-\boldsymbol{Q}_T)^{-1}$ quantifies the expected time spent in each transient state before absorption. Each entry N_{ij} represents the expected duration the system remains in state j starting from state i, offering a detailed view of the system's temporal dynamics under repeated hazard exposure.

Based on this formulation, a suite of resilience metrics can be systematically derived to characterize system performance. The expected lifetime before collapse, assuming the system starts in the undamaged state (DS_0), is:

$$\tau_0 = \sum_j N_{0j}, \tag{6}$$

which captures the system's average operational duration prior to failure.

From this, we define the resilience index as:

$$\mathcal{R}_i = \frac{N_{i0}}{\tau_0}, \tag{7}$$

representing the fraction of time the system spends in the undamaged state relative to its expected lifetime. This index reflects the system's capacity to preserve full functionality throughout its service life.

To facilitate interpretation and enable comparisons across different systems or recovery strategies, a resilience score is introduced as

$$\beta_i = \Phi^{-1}(\mathcal{R}_i), \tag{8}$$

where Φ^{-1} denotes the inverse standard normal cumulative distribution function. This transformation maps resilience onto a standardized Z-score scale, providing a familiar statistical context for engineers and risk analysts.

Besides, this formulation enables intuitive interpretation of resilience, facilitating comparisons across systems and recovery strategies within a probabilistic performance-based framework.

3. Case Study/Benchmark: steel MRF for critical infrastructure

In this section, we illustrate the application of the proposed framework using a benchmark case study inspired by the European SPIF project, presented in Butenweg et al. (2021), Butenweg et al. (2020). For brevity and illustrative purposes, we consider here already derived state-dependent fragility functions from Nardin (2022), Nardin et al. (2024). By definition, state-dependent fragilities are a class of fragilities conditioned not only on the seismic intensity measure (IM) but also on the initial damage state, capturing the structure's evolving vulnerability. Full methodological details can be found in Nardin et al. (2025) and Nardin et al. (2024).

The benchmark structure is a full-scale, three-storey steel moment-resisting frame (MRF) designed for critical infrastructure, characterized by a flexible diaphragm and integrated with process components such as piping systems, bolted flange joints (BFJs), electrical cabinets, and storage tanks. The structural model, developed in SAP2000 Computers and Structures Inc. (2023) and calibrated against shake table experiments at EUCENTRE, is equipped with reduced-order models for non-structural elements to balance fidelity and computational efficiency Quinci et al. (2023). To capture the structure's performance degradation across multiple seismic events, nonlinear time history analyses (NLTHAs) were carried out under various initial damage states. Due to the high computational demand, a limited set of simulations was used to train polynomial chaos expansion (PCE) surrogate models with the UQLab software Marelli and Sudret (2014), enabling efficient Monte Carlo simulations.

The resulting fragility functions are defined for the maximum inter-storey drift ratio, following FEMA 356 performance thresholds: DS_0, Immediate Occupancy (IO) at 0.7% drift; DS_1, Life Safety (LS) at 2.5% drift; and DS_2 Collapse Prevention (CP) at 5% drift.

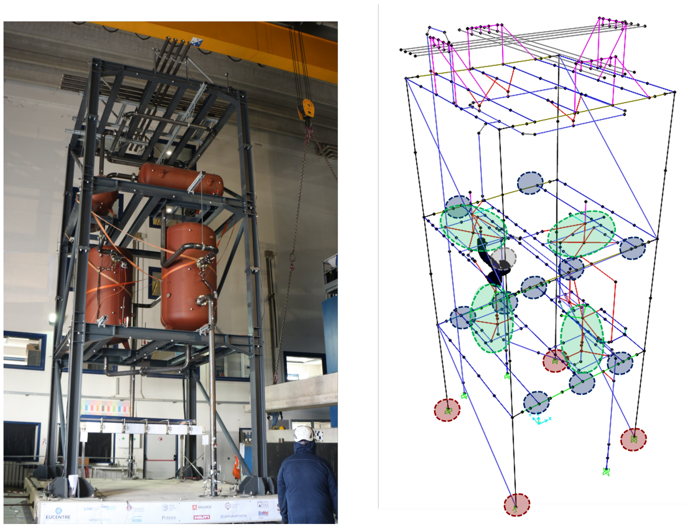

(a) (b)

Fig. 3. (a) Photo of the full-scale SPIF case study at the EUCENTRE facility and (b) its SAP2000 model, as described in Quinci et al. (2023).

Figure 4 presents the fragility curves associated with these limit states. Formally:

$$\mathbb{P}[DS_j \mid DS_i, IM = im] = \mathbb{P}[DS \geq ds_j \mid DS_i, im], \tag{9}$$

where the transition probability depends on both the current damage state (DS_i) and the seismic intensity level.

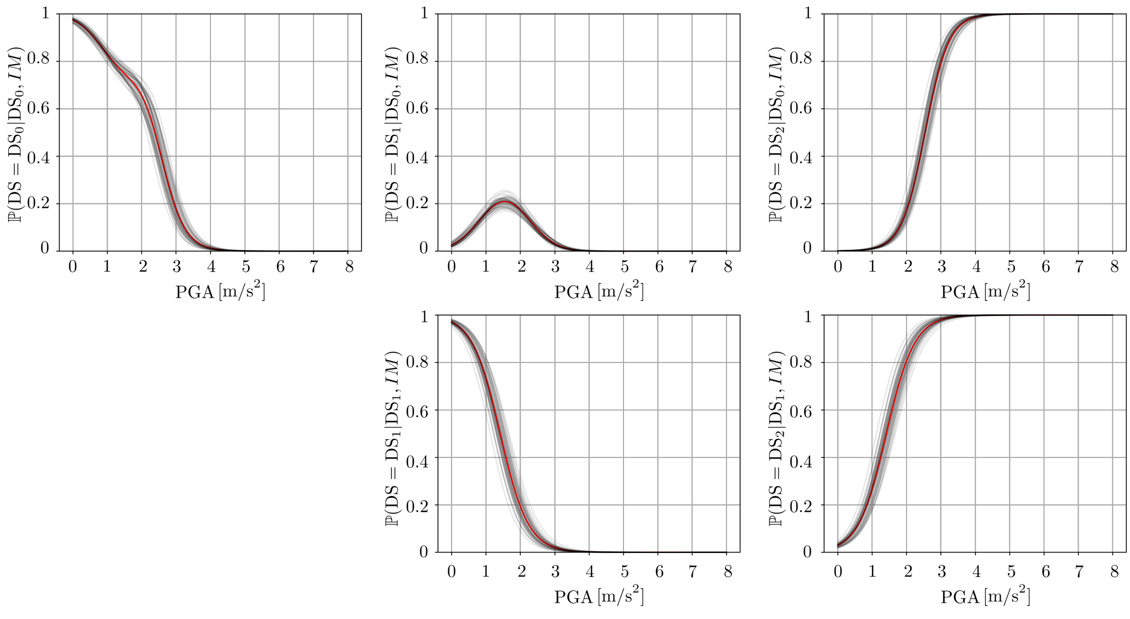

Fig. 4. Seismic fragility curves considered, from Nardin (2022).

In addition, to reflect a realistic seismic risk context, three Italian site-specific hazard intensity levels were considered, each representing distinct ground motion severity scenarios: (i) low seismic zone, located in Northern Italy, Milano; (ii) medium and (iii) severe seismicity, located in center Italy, Palmoli and L'Aquila, respectively. The annual PGA exceedance hazard rate and their 16^{th}-50^{th}-84^{th} quantile are reported in Figure 5, based on data provided by the INGV website (https://esse1-gis.mi.ingv.it/).

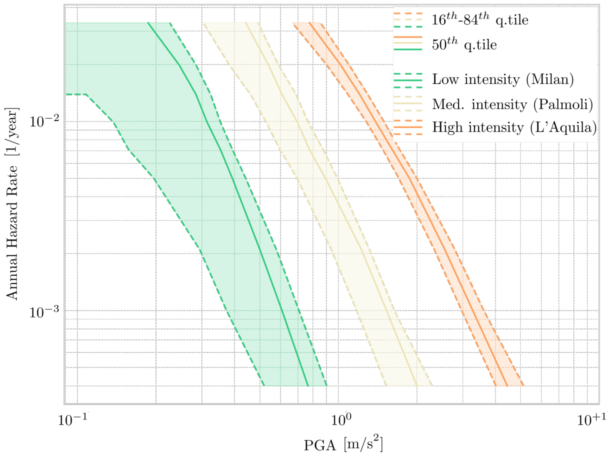

Fig. 5. Annual hazard rate for three locations in Italy with different levels of seismicity.

4. Discussion of results and model comparison

Building on the state-dependent fragilities, recovery rates, and seismicity data presented in the previous section, we derive both the full-state probability distribution of the complete $\boldsymbol{Q}$ matrix (as defined in Eq. (2)-(3)) and the spectral analysis results of the reduced matrix $\boldsymbol{Q_T}$, as discussed in Section 2.

Figure 6 illustrates the time-evolving probability distribution across the three possible damage states, assuming a life-span (T_{Life}) of 500 years and a a fixed and unrealistically high recovery rate μ_{01} of 10^2, intentionally set as an extreme value to evaluate model sensitivity. Here, DS_2 is treated as an absorbing state, and only μ_{01} is non-zero since transitions from DS_2 are physically not allowed.

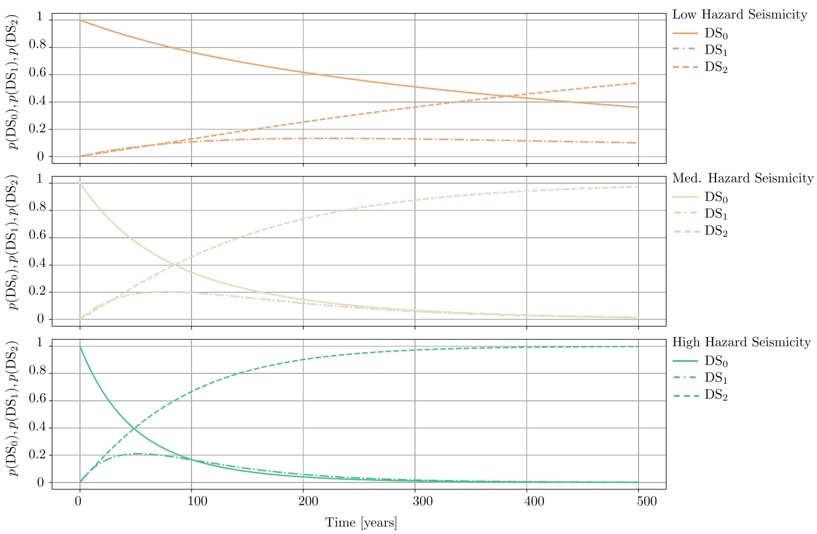

Fig. 6. Time-evolving probability distribution $\mathbb{P}(\text{DS}_0), \mathbb{P}(\text{DS}_1), \mathbb{P}(\text{DS}_2)$ for the low, medium, and high seismicity hazard considered.

Despite the high recovery rate, the system ultimately reaches the absorbing state DS_2. What changes across scenarios is how quickly this occurs, depending on the seismic hazard level. Under low seismicity, it takes nearly 400 years for the probability of being in DS_2 to exceed that of remaining in a non-collapse state. In contrast, in higher seismicity regions, this transition occurs much faster, shifting to the left on the time axis down to 100 or even around 50 years for the highest hazard levels.

To evaluate the reliability of the system, however, we must focus on the submatrix $\boldsymbol{Q_T}$. Figure 7 presents how the system reliability, quantified by β, varies with the recovery rate μ_{01} under three distinct seismic hazard scenarios.

The results reveal a clear threshold behavior: below a certain recovery rate, the system's reliability remains largely unaffected. However, once recovery becomes sufficiently effective to counterbalance the damage progression driven by seismicity, reliability improves markedly. This indicates the critical role of recovery policies in mitigating long-term degradation and sustaining structural performance over time.

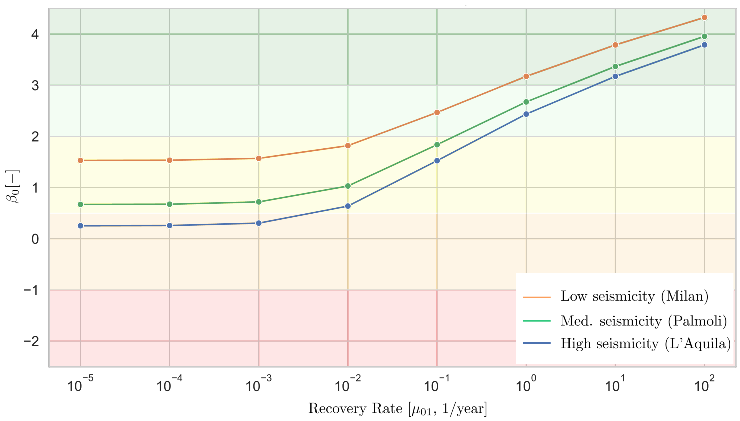

Fig. 7. System reliability as a function of recovery rates.

5. Conclusions and outlook

This work introduces a novel recovery-aware extension of the PBEE framework, offering a dynamic and probabilistic view of seismic risk through the lens of state evolution and recovery. By coupling CTMC modeling with state-dependent fragility functions and scalable uncertainty quantification tools, the proposed framework enables robust resilience metrics that account for both degradation and recovery. The application to a full-scale industrial structure demonstrates its relevance for critical infrastructure, particularly in high-seismic-risk contexts. Looking ahead, this methodology opens pathways for integrating adaptive recovery strategies, region-specific data, and system interdependencies: crucial elements for future-ready, resilience-informed design and policy.

Acknowledgements

This research is supported by the Marie-Sklodowska Curie program and the REACTIS project, GA no. 101147351. Views and opinions expressed are however those of the authors only and do not necessarily reflect those of the European Union, or REA or any sponsor. Neither the European Union nor the granting authority can be held responsible for them.

References

FEMA and NIST, 2021. Recommended Options for Improving the Built Environment for Post-Earthquake Reoccupancy and Functional Recovery Time. FEMA P-2090 / NIST SP-1254, January. Available at: https://www.fema.gov/sites/default/files/documents/fema_p2090-nist-sp1254-functional-recovery.pdf.

Almufti, I., Willford, M., 2013. REDi™ Rating System: Resilience-based Earthquake Design Initiative for the Next Generation of Buildings. DOI: 10.13140/RG.2.2.20267.75043.

Terzic, V., Villanueva, P.K., Saldana, D., Yoo, D.Y., 2021. F-Rec Framework: Novel Framework for Probabilistic Evaluation of Functional Recovery of Building Systems. PEER Report 2021-06, Pacific Earthquake Engineering Center.

Nardin, C., Marelli, S., Bursi, O.S., Sudret, B., Broccardo, M., 2025. UQ state-dependent framework for seismic fragility assessment of industrial components. Reliability Engineering & System Safety 261, 111067. DOI: 10.1016/j.ress.2025.111067.

FEMA, 2000. Prestandard and Commentary for the Seismic Rehabilitation of Buildings. FEMA 356, Federal Emergency Management Agency, Washington, D.C., USA. Available at: https://www.fema.gov/sites/default/files/2020-07/fema_356.pdf.

Marelli, S., Sudret, B., 2015. UQLab: A framework for uncertainty quantification in MATLAB. ETH Zurich. UQLab user manual – PCE module, Version 1.3. Available at: https://www.uqlab.com.

Marelli, S., Sudret, B., 2014. UQLab: A framework for uncertainty quantification in MATLAB. In: Vulnerability, Uncertainty, and Risk: Quantification, Mitigation, and Management, pp. 2554–2563.

Nardin, C., 2022. Seismic Experimental Analyses and Surrogate Models of Multi-Component Systems in Special-Risk Industrial Facilities. PhD thesis, Università degli Studi di Trento, Trento, Italy.

Butenweg, C., Bursi, O.S., Nardin, C., Lanese, I., Pavese, A., Marinković, M., Paolacci, F., Quinci, G., 2021. Experimental Investigation on the Seismic Performance of a Multi-Component System for Major-Hazard Industrial Facilities. Proceedings of the ASME Pressure Vessels and Piping Conference. DOI: 10.1115/PVP2021-61696.

Butenweg, C., Marinković, M., Pavese, A., Lanese, I., Parisi, E., Hoffmeister, B., Pinkawa, M., Vulcu, C., Bursi, O.S., Nardin, C., Paolacci, F., Quinci, G., Fragiadakis, M., Weber, F., Huber, P., Renault, P., Gündel, M., Dyke, S., Ciuccu, M., Marino, A., 2020. Seismic performance of multiple-component systems in special risk industrial facilities. In: *Proceedings of the 17th World Conference on Earthquake Engineering (17WCEE)*, Sendai, Japan.

Nardin, C., Bursi, O.S., Broccardo, M., Marelli, S., Sudret, B., 2024. State-dependent seismic fragility functions for vertical tanks installed on major hazard industrial substructure module. In: *Proceedings of the 18th World Conference on Earthquake Engineering (18WCEE)*, Milan, Italy, July 2, 2024.

Quinci, G., Nardin, C., Paolacci, F., Bursi, O.S., 2023. Modelling of Non-Structural Components of an Industrial Multi-Storey Frame for Seismic Risk Assessment. Bulletin of Earthquake Engineering 21, 6065–6089. DOI: 10.1007/s10518-023-01753-4.

Computers and Structures, Inc., 2023. SAP2000: Integrated Software for Structural Analysis and Design. Version 25, Walnut Creek, California, USA. Available at: https://www.csiamerica.com/products/sap2000.

Pacor, F., Ameri, G., Bindi, D., Luzi, L., Massa, M., Paolucci, R., Smerzini, C., 2009. Characteristics of strong ground motions from the L'Aquila (Mw = 6.3) earthquake and its strongest aftershocks. Bulletin of Earthquake Engineering. Istituto Nazionale di Geofisica e Vulcanologia, Milano, and Politecnico di Milano.

Bagagli, M., Valoroso, L., Michelini, A., Cianetti, S., Gaviano, S., Giunchi, C., Jozinović, D., Lauciani, V., 2023. AQ2009 – The 2009 Aquila Mw 6.1 earthquake aftershocks seismic dataset for machine learning application. Istituto Nazionale di Geofisica e Vulcanologia (INGV). DOI: 10.13127/ai/aquila2009.

Trivedi, K.S., Bobbio, A., 2017. Reliability and Availability Engineering: Modeling, Analysis, and Applications. Cambridge University Press, Cambridge.

Ouyang, M., Dueñas-Osorio, L., 2012. Time-dependent resilience assessment and improvement of urban infrastructure systems. Chaos: An Interdisciplinary Journal of Nonlinear Science 22(3), 033122. DOI: 10.1063/1.4737204.